Electronic Supplementary Information

Magnetic grinding synthesis of copper sulfide based photocatalytic composites for degradation of organic dyes under visible light

Zhangbin Song[a], Yan Liu*[a], Bin Zhang[a], Shasha Song[a], Zhen Zhou[a], Yaoguo Huang[a] and Zengdian Zhao*[a]

[a]School of Chemistry and Chemical Engineering, Shandong University of Technology, Zibo 255049, China.

Corresponding author:
*Yan Liu e-mail: liuyan@sdut.edu.cn
Zengdian Zhao e-mail: zhaozengdian@sdut.edu.cn

Table of contents

1. Experimental section

1.1 Material synthesis

Other materials, CuS, ZnS, CdS and CuS/CdS were prepared according to the CuS/ZnS synthetic conditions. Binary metal sulfide CuS, ZnS and CdS were synthesized by mixing the corresponding metal substance and sulfur powder in the grinding tank. The molar ratio of metal to sulfur powder is 1:1 and the mass ratio of grinding medium to material is 20:1. Reactant grinding for 5 h at working frequency of 50 Hz.

Synthetic raw material of CuS/CdS composite is copper powder, cadmium powder and sulfur powders with molar ratio 1:1:2. The mass ratio of grinding medium to added precursor materials is 20:1. Reactant grinding for 5 h at the working frequency of 50 Hz.

1.2 Characterization techniques

The crystal phases of the products were characterized by powder X-ray diffraction (XRD) (Bruker D8 ADVANCE) with Cu-Kα irradiation at 20 kV. The chemical composites of the samples were analyzed by X-ray photoelectron spectroscopy (XPS, Thermo Fisher ESCALAB XI+). The morphology, microstructure and element mapping of the obtained products were measured with microscopy (SEM) (Thermo Fisher) equipped with an energy dispersive X-ray (EDS) spectrometer operating at 20 kV and transmission electron microphology (TEM) (FEI Systems) spectrometer operating at 200 kV. Fourier translation infrared (FT-IR) spectra of as synthesized products was studied over the range of 4000-400 cm-1 using FT-IR spectrometer (WQF-530). The Brunaure-Emmett-Teller (BET) specific surface areas of the products were measured by nitrogen (N_2) adsorption-desorption at 300 K (ASAP 2460). Photoluminescence (PL) spectrum was obtained in Steady-state fluorescence spectrometer (Hitachi F-4700). UV–vis Diffuse Reflectance spectrum (DRS) was obtained with standard $BaSO_4$ method for obtaining energy band and light absorption information of the material in SHIMADZU UV2600 spectrophotometer. UV-vis spectrophotometer (Agilent Cary 60) was used to observe concentration of MB, RhB and MO. The total organic carbon content (TOC) was detected by a total organic carbon analyzer (vario TOC).

1.3 Photocatalytic studies

Photocatalytic degradation efficiency is defined as follows:[1]

$$\text{Dffegradation eiciency (\%)} = (1-C_t/C_0)\times 100\% \quad \text{(S1)}$$

Where, C_0 and C_t represents the concentration of the organic dye solution at the adsorption-desorption equilibrium and the concentration at different irradiation time, respectively.

The photocatalytic degradation rate of dyes were estimated at solid-liquid interface using a Langmuir-Hinshelwood pseudo-first order kinetic expression as mentioned follows:[2]

$$\ln (C_0/C_t) = kt \quad \text{(S2)}$$

In order to investigate the stability of photocatalyst, taking the CuS/ZnS and CuS/CdS composites as a representative, the stability of its degradation of MB aqueous solution was explored. Collect the catalyst after the photocatalysis and add 50 mL new MB aqueous solution with a concentration of 15 mg/L. Repeat the photocatalysis experiment for 4 times. The stability of prepared composites was evaluated by comparing the degradation effect of MB aqueous solution during the cycle.

2. Mulliken electronegativity theory

In general, the potentials of the conduction band (CB) and valence band (VB) edges of CuS, ZnS and CdS were determined by adopting the well-known Mulliken electronegativity theory:[3]

$$E_{CB} = \chi - E_e - 0.5E_g \quad \text{(S3)}$$

$$E_e = 4.5 \text{ eV} \quad \text{(S4)}$$

$$E_{VB} = E_{CB} + E_g \quad \text{(S5)}$$

Where, E_{CB} is the conduction band edge potential, χ denotes the electronegativity of the semiconductors, which is expressed as the geometric mean of the absolute electronegativity of the constituent atoms present in the semiconductor and the electronegativity is calculated as the arithmetic mean of the atomic electron affinity and first ionization energy. The reported χ values of CuS, ZnS and CdS are ca. 5.27 eV, 5.26 eV and 5.05 eV, respectively, and E_g is the energy of the free electrons on the hydrogen scale, which is 4.5 eV.[4,5] E_g is the band gap of the semiconductor.

According to the UV-vis spectra and Tauc approach, we can obtain the band gaps of CuS, ZnS and CdS. Therefore, according to this formula, we can obtain the energy band edge level of semiconductor photocatalyst.

3. Figures and Tables

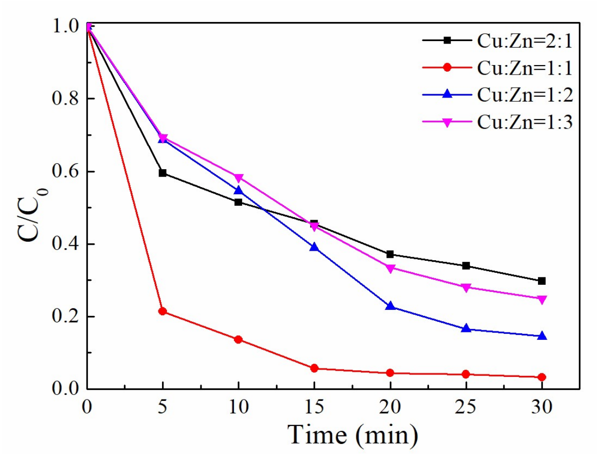

Fig. S1 Comparison of photocatalytic activities of different molar rations for MB degradation.

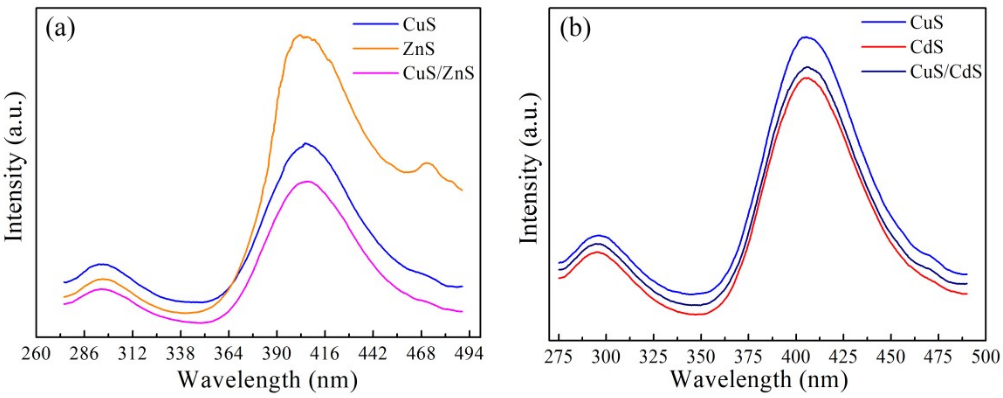

Fig. S2 PL spectra of (a) CuS, ZnS, CuS/ZnS and (b) CuS, CdS, CuS/CdS.

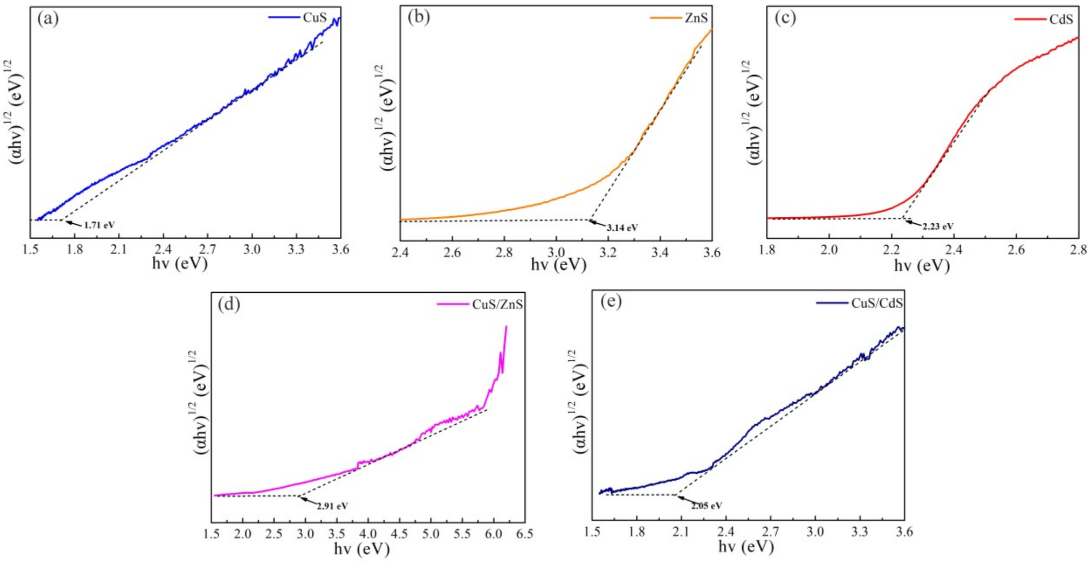

Fig. S3 Band gap plots of (a) CuS, (b) ZnS, (c) CdS, (d) CuS/ZnS and (e) CuS/CdS as Tauc plots for estimation.

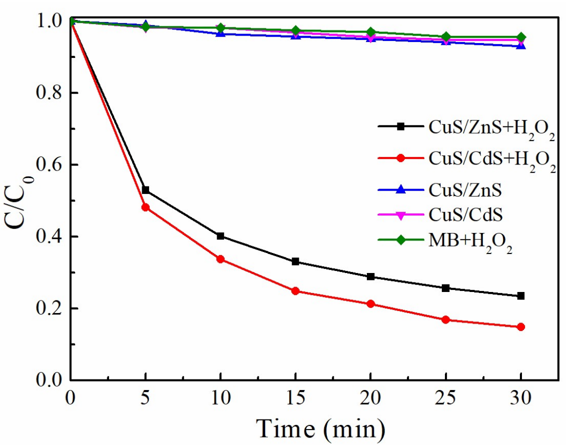

Fig. S4 CuS/ZnS and CuS/CdS composites degrade MB in the dark condition.

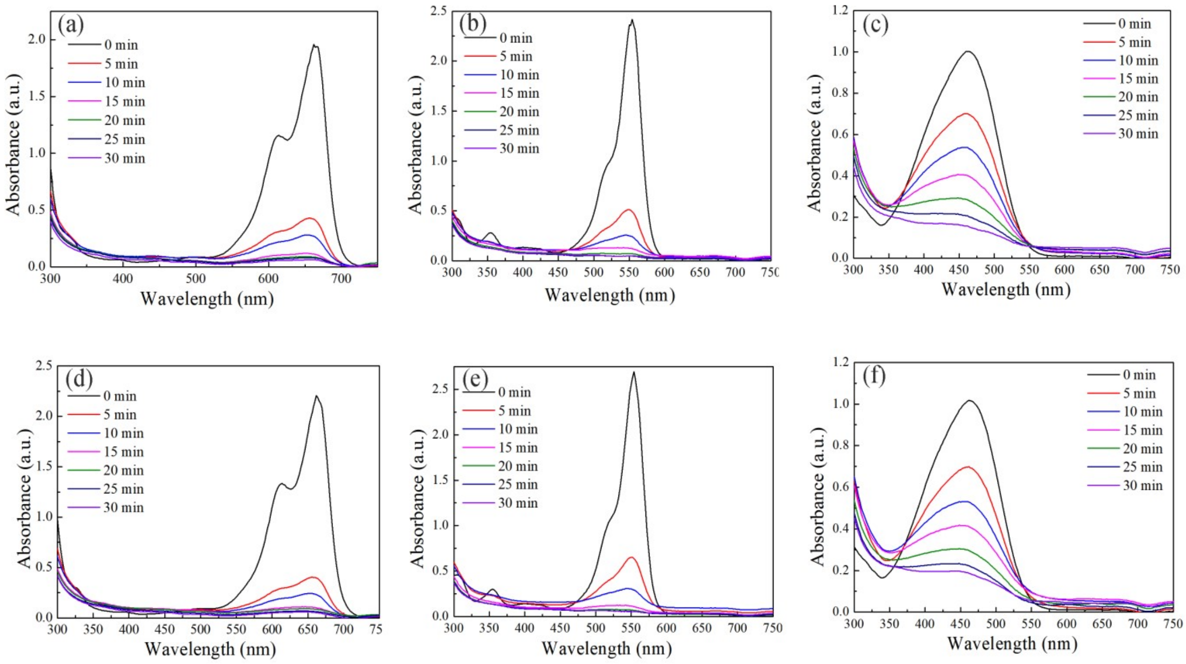

Fig. S5 UV adsorption spectra of MB, RhB and MO (a-c) CuS/ZnS, (d-f) CuS/CdS.

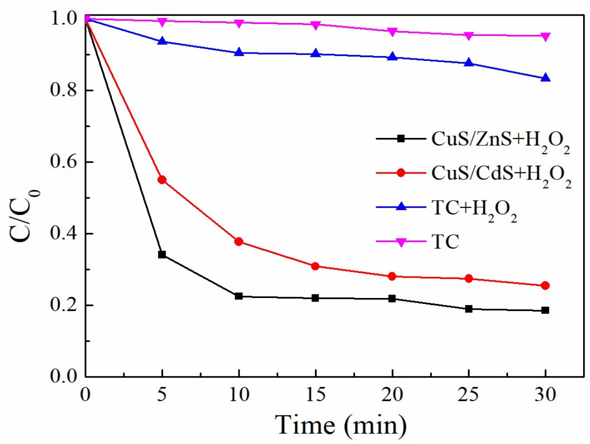

Fig. S6 CuS/ZnS and CuS/CdS composites degrade tetracycline (TC).

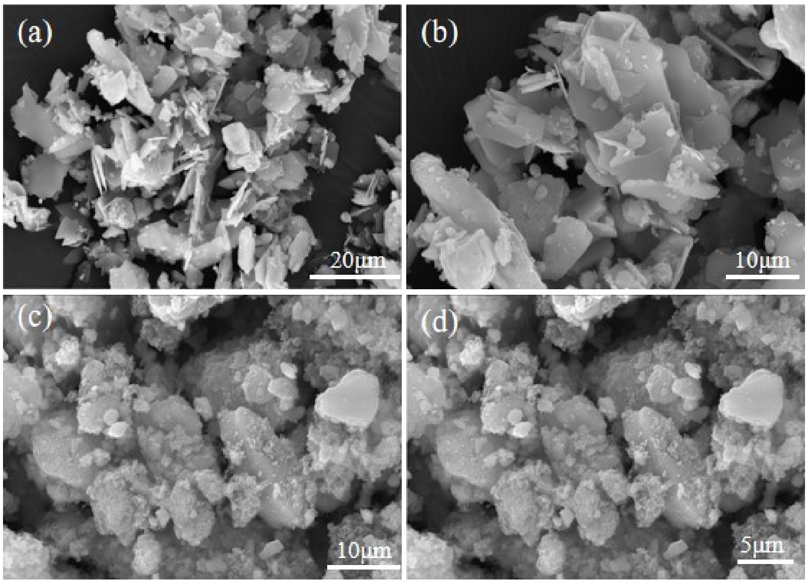

Fig. S7 SEM images of (a) CuS/ZnS and (b) CuS/CdS after recycling.

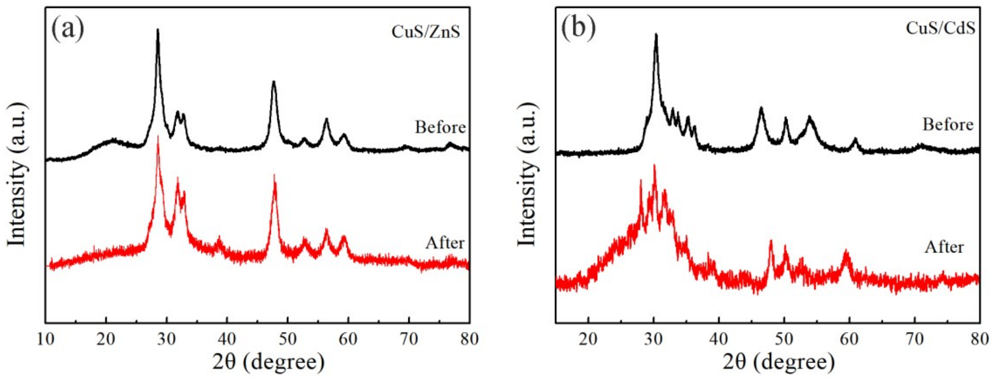

Fig. S8 XRD patterns of (a) CuS/ZnS and (b) CuS/CdS after cycling.

Table S1 BET surface areas and pore volumes of CuS, ZnS, CdS, CuS/ZnS and CuS/CdS.

	S_{BET}(m^2/g)	V_{pore}(cm^3/g)	D_{pore}(nm)
CuS	1.7945	0.011434	28.0422
ZnS	19.5852	0.067396	12.2789
CdS	9.0276	0.033755	12.9270
CuS/ZnS	3.6297	0.014217	12.8491
CuS/CdS	5.4593	0.071322	13.2057

Table S2 Observed pseudo-first order rate constants, R^2 values, maximum degradation (%) of samples.

Dye	Samples	Dye Degradation Efficiency (%)	Rate Constant (min^{-1})	(R^2) value
	CuS	83.19	0.06483	0.9859
	ZnS	32.46	0.01609	0.9017
	CdS	28.43	0.01355	0.9258
MB	CuS/ZnS	96.74	0.13864	0.9389
	CuS/CdS	97.70	0.1520	0.9391
	MB	8.67	0.00359	0.9265
	MB (no H_2O_2)	6.63	0.00267	0.9365
	CuS	97.52	0.11976	0.9974
	ZnS	29.26	0.01269	0.9719
	CdS	25.83	0.0114	0.9705
RhB	CuS/ZnS	98.04	0.15927	0.9544
	CuS/CdS	97.97	0.16035	0.9526
	RhB	8.17	0.00277	0.9809
	RhB (no H_2O_2)	5.43	0.00177	0.9797
	CuS	84.93	0.02266	0.9901
	ZnS	28.03	0.00351	0.9962
	CdS	19.23	0.00267	0.9569
MO	CuS/ZnS	89.00	0.02631	0.9981
	CuS/CdS	84.88	0.02322	0.9897
	MO	7.87	0.00111	0.8910
	MO (no H_2O_2)	1.53	0.00016	0.9763

Table S3 Comparison of the CuS/ZnS and CuS/CdS photocatalysts for the dye degradation comparable with the other CuS-based photocatalysts.

S. No.	Material	Synthesis route	Illumination source	Target dye	Time (min)	Dye deg. (%)	Ref. no.
1	CuS/ZnS	hydrothermal	Xenon Lamp	RhB	60	98	6
2	CuS/ZnS	Hydrothermal	Xenon Lamp	MB	5	95	7
3	CuS/ZnS	Solvo/hydrothermal	Ultraviolet Light	MB	150	93	8
4	CuS/CdS	Solvothermal	Xenon Lamp	MB	150	100	9
5	CuS/ZnO	Wet-chemical	Solar + Ultrasonic	MB	20	98	10
6	CuS/TiO_2	Bifunctional link molecule	Xenon Lamp	RhB	90	69	11
7	CuS/ZnS, CuS/CdS	Mechanochemical	Xenon Lamp	MB, RhB, MO	30,90	97 and 85	Present work

Table S4 Total organic carbon content removal efficiency of CuS/ZnS and CuS/CdS composites.

		TC-IC (mg/L)				
		first	second	Average value	TOC	Removal efficiency
CuS/ZnS	TC	4.600	4.775	4.688	4.688	53.70%
	IC	0	0	0		
CuS/CdS	TC	6.115	6	6.058	6.056	40.17%
	IC	0	0	0		
MB	TC	10.183	10.064	10.124	10.124	————
	IC	0	0	0		

4. References

1 S. Harish, M. Navaneethan, J. Archana, A. Silambarasan, S. Ponnusamy, C. Muthamizhchelvan and Y. Hayakawa, Controlled synthesis of organic ligand passivated ZnO nanostructures and their photocatalytic activity under visible light irradiation, *Dalton T.,* 2015, **44**, 10490-10498.

2 J. Yu and L. Qi, Template-free fabrication of hierarchically flower-like tungsten trioxide assemblies with enhanced visible-light-driven photocatalytic activity, *J. Hazard. Mater.*, 2009, **169**, 221-227.

3 J. Liu, Origin of High Photocatalytic Efficiency in Monolayer g-C_3N_4/CdS Heterostructure: A Hybrid DFT Study, *J. Phys. Chem. C,* 2015, **119**, 28417-28423.

4 C. Mondal, A. Singh, R. Sahoo, A. K. Sasmal, Y. Negishi and T. Pal, Preformed ZnS nanoflower prompted evolution of CuS/ZnS p–n heterojunctions for exceptional visible-light driven photocatalytic activity, *New J. Chem.,* 2015, **39**, 5628-5635.

5 W. Cui, W. An, L. Liu, J. Hu, Y. Liang, Synthesis of CdS/BiOBr composite and its enhanced photocatalytic degradation for Rhodamine B, *Appl. Surf. Sci.,* 2014, **319**, 298-305.

6 X. Wang, Y. Li, M. Wang, W. Li, M. Chen and Y. Zhao, Synthesis of tunable ZnS-CuS microspheres and visible-light photoactivity for rhodamine B, *New J. Chem.*, 2014, **38**, 4182-4189.

7 S. Harish, J. Archana, M. Navaneethan, S. Ponnusamy, A. Singh, V. Gupta, D. K. Aswal, H. Ikeda and Y. Hayakawa, Synergetic effect of CuS@ZnS nanostructures on photocatalytic degradation of organic pollutant under visible light irradiation, *RSC Adv.*, 2017, **7**, 34366-34375.

8 S. Shahi, S. Saeednia, P. Iranmanesh and M. H. Ardakani, Influence of synthesis parameters on the optical and photocatalytic properties of solvo/hydrothermal CuS and ZnS nanoparticles, *Luminescence*, 2021, **36**, 180-191.

9 N. X. Liu, W. L. Fu, C. Chen, M. C. Liu, F. Xue, Q. H. Shen and J. C. Zhou, Controlling the core–shell structure of CuS@ CdS heterojunction via seeded growth with tunable photocatalytic activity, *ACS Sustain. Chem. Eng.*, 2018, **6**, 15867–15875.

10 D. Y. Hong, W. L. Zang, X. Guo, Y. M. Fu, H. X. He, J. Sun, L. L. Xing, B. D. Liu and X. Y. Xue, High piezo-photocatalytic efficiency of CuS/ZnO nanowires co-using solar and mechanical energy for degrading organic dye, *ACS Appl. Mater. Inter.*, 2016, **8**, 21302–21314.

11 S. Y. Yu, J. C. Liu, Y. Zhou, R. D. Webster and X. L. Yan, Effect of synthesis method on the nanostructure and solar-driven photocatalytic properties of TiO_2-CuS composites, *ACS Sustain. Chem. Eng.*, 2017, **5**, 1347–1357.